PROCEEDINGS A

royalsocietypublishing.org/journal/rspa



Research





Cite this article: Cui S, Pelinovsky DE. 2025 Instability bands for periodic travelling waves in the modified Korteweg—de Vries equation. *Proc. R. Soc. A* **481**: 20240993. https://doi.org/10.1098/rspa.2024.0993

Received: 26 December 2024 Accepted: 27 June 2025

Subject Areas:

applied mathematics, fluid mechanics

Keywords:

modified Korteweg—de Vries equation, periodic travelling wave, modulational instability

Author for correspondence:

Dmitry E. Pelinovsky e-mail: pelinod@mcmaster.ca

Electronic supplementary material is available online at https://doi.org/10.6084/m9.figshare. c.7947832.

THE ROYAL SOCIETY PUBLISHING

Instability bands for periodic travelling waves in the modified Korteweg—de Vries equation

Shikun Cui^{1,2} and Dmitry E. Pelinovsky²

¹School of Mathematical Sciences, Dalian University of Technology, Dalian 116024, People's Republic of China ²Department of Mathematics and Statistics, McMaster University,

DEP, 0000-0001-5812-440X

Hamilton L8S 4K1, Ontario, Canada

Two families of periodic travelling waves exist in the focusing modified Korteweg-de Vries equation. Spectral stability of these waveforms with respect to co-periodic perturbations of the same period has been previously explored by using spectral analysis and variational formulation. By using tools of integrability, such as a relation between squared eigenfunctions of the Lax pair and eigenfunctions of the linearized stability problem, we revisit the spectral stability of these waveforms with respect to perturbations of arbitrary periods. In agreement with previous works, we find that one family is spectrally stable for all parameter configurations, whereas the other family is spectrally unstable for all parameter configurations. We show that the onset of the co-periodic instability for the latter family changes the instability bands from figure-8 (crossing at the imaginary axis) into figure- ∞ (crossing at the real axis).

1. Introduction

Instabilities of steadily propagating waves on a fluid surface, called Stokes waves, have been recently explored in many computational details due to advanced numerical algorithms with high precision and accuracy [1–6]. As the Stokes wave gets a larger height and higher steepness, the spectral problem for co-periodic perturbations admits more unstable eigenvalues which

© 2025 The Authors. Published by the Royal Society under the terms of the Creative Commons Attribution License http://creativecommons.org/licenses/by/4.0/, which permits unrestricted use, provided the original author and source are credited.

bifurcate from the origin due to coalescence of pairs of purely imaginary eigenvalues and splitting into pairs of real eigenvalues [4]. At the same time, the spectral problem for perturbations of arbitrary periods display more complicated patterns of instability bands with multiple loops on the purely imaginary and real axes [3,5]. The figure-8 instability (crossing at the imaginary axis), which is standard in the limit of small amplitudes [7–10] transforms into the figure- ∞ instability (crossing at the real axis) with further exchanges between co-periodic and anti-periodic eigenvalues as eigenvalues of the dominant instability [1,2]. It was conjectured that the recurrent exchange between these patterns is universal near the limit to the periodic wave with the maximal height and occurs in other wave models such as the Whitham equation [11].

This motivating picture related to the Stokes waves in Euler's equations calls for a more systematic investigation of the spectral instability of periodic travelling waves in the basic fluid models such as the focusing modified Korteweg–de Vries (mKdV) equation. The spectral stability of periodic travelling waves in this model has been studied in many details by using tools of integrability [12–18] and functional analysis [19–26]. The purpose of this work is to give a complete picture of the spectral stability of the general periodic travelling waves to perturbations of all periods and to show that the onset of the co-periodic instability changes the instability bands from figure-8 to figure- ∞ .

We will describe the state-of-the-art and present the main results by using the standard form of the focusing mKdV equation,

$$u_t + 6u^2u_x + u_{xxx} = 0, (1.1)$$

where subscripts x and t represent the partial derivatives in the spatial and temporal variables, respectively, and where u=u(x,t) is real. The initial-value problem for the mKdV equation (1.1) is globally well-posed in the energy space H^1 both on $\mathbb R$ and in the periodic domain [27]. It was further proven in [28] that the global well-posedness can be extended to the Sobolev spaces of low regularity in H^s for $s>\frac14$ on $\mathbb R$ and H^s for $s>\frac12$ in the periodic domain. By using integrability, the global well-posedness of the mKdV equation was extended to H^s for $s>-\frac12$ on $\mathbb R$ [29].

The travelling wave of the mKdV equation (1.1) with the spatial profile $U(x) : \mathbb{R} \to \mathbb{R}$ is given by u(x,t) = U(x-ct), where c is the wave speed. The wave profile U satisfies the third-order equation

$$U''' + 6U^2U' - cU' = 0, (1.2)$$

which is integrated into the second-order equation

$$U'' + 2U^3 - cU = b (1.3)$$

with the integration constant *b*. Two particular waveforms for the periodic travelling waves were studied in many details:

$$U(x) = dn(x, k), \quad c = 2 - k^2, \quad b = 0$$
 (1.4)

and

$$U(x) = k \operatorname{cn}(x, k), \quad c = 2k^2 - 1, \quad b = 0,$$
 (1.5)

where k is elliptic modulus, $k \in (0,1)$, and the Jacobi elliptic functions have been used. We shall refer to equations (1.4) and (1.5) as the dnoidal and cnoidal waves, respectively. With the use of the scaling transformation

$$u(x,t)\mapsto \alpha u(\alpha x,\alpha^3 t),\quad \alpha>0$$

and the translational symmetries

$$u(x,t) \mapsto u(x + x_0, t + t_0), \quad x_0, t_0 \in \mathbb{R},$$

these two waveforms extend to all possible travelling periodic wave solutions of the second-order equation (1.3) with b = 0.

- the dnoidal wave (1.4) is spectrally stable to co-periodic perturbations for all $k \in (0,1)$, and
- the cnoidal wave (1.5) is spectrally stable to co-periodic perturbations for $k \in (0, k_*)$ and spectrally unstable for $k \in (k_*, 1)$, where $k_* \approx 0.909$.

Furthermore, it was shown in [21,22] that

- the dnoidal wave (1.4) is modulationally stable to long periods for all $k \in (0, 1)$, and
- the cnoidal wave (1.5) is modulationally unstable to long periods for all $k \in (0, 1)$.

Regarding the periodic travelling waves with $b \neq 0$, stability of one particular solution was proven in [30]. Two continuous families exist for $b \neq 0$ [13,15] which extend the dnoidal and cnoidal waves (equations (1.4) and (1.5)), see equations (2.4) and (2.6). Stability of these waveforms with respect to co-periodic perturbations has been systematically studied in [24,25] by using minimization of the quadratic form

$$\oint [(u')^2 + cu^2] \, \mathrm{d}x$$

subject to fixed mean value $\oint u dx = m$ and the fixed L^4 norm $\oint u^4 dx = 1$ (see review in [31]).

- Under the zero-mean constraint, m = 0, the cnoidal wave (1.5) is a minimizer of the constrained variational problem for $k \in (0, k_*)$ and a saddle point for $k \in (k_*, 1)$ with two symmetric minimizers bifurcating at $k = k_*$ in the supercritical pitchfork bifurcation [25].
- Under a fixed non-zero mean value, $m \neq 0$, the imperfect pitchfork bifurcation breaks one branch of global minimizers of the constrained variational problem away from the other two branches, one of which is a saddle point and the other one is a local minimizer [24]. The local and global minimizers are spectrally stable to co-periodic perturbations and the saddle points are spectrally unstable for all parameter values [24]. Furthermore, the local and global minimizers are realized with both solution waveforms (equations (2.4) and (2.6)), whereas the saddle points are only realized by the waveform (2.6) [24].

Next, we present the main results of this work in relation to the state-of-the-art.

- First, we show by using the relation between squared eigenfunctions satisfying the Lax pair and eigenfunctions of the spectral stability problem that the solution waveform (2.4) generalizing dnoidal waves (1.4) is spectrally stable for all parameter configurations and the solution waveform (2.6) generalizing cnoidal waves (1.5) is spectrally unstable for all parameter configurations. This agrees with theorem 2 in [21] where modulational stability of the solution waveforms was studied to perturbations of long periods.
- Second, we show that the spectral instability of the solution waveform (2.6) to co-periodic perturbations triggers a transformation of figure-8 before the co-periodic instability to figure- ∞ after the co-periodic instability. This conclusion agrees with the modulational stability theory in [21] and numerical approximations (see fig. 1 in [21]) but has not been described in precise detail. The analytical study of the co-periodic stability in [23] was accompanied by numerical approximations (see fig. 1 in [23]), which showed some transformations of figure-8 before figure- ∞ was attained. The stability spectrum of the dnoidal and cnoidal waves was computed numerically in [14] for just one value of $k \in (0,1)$, for which only figure-8 was obtained and the transformation to figure- ∞ was missed.

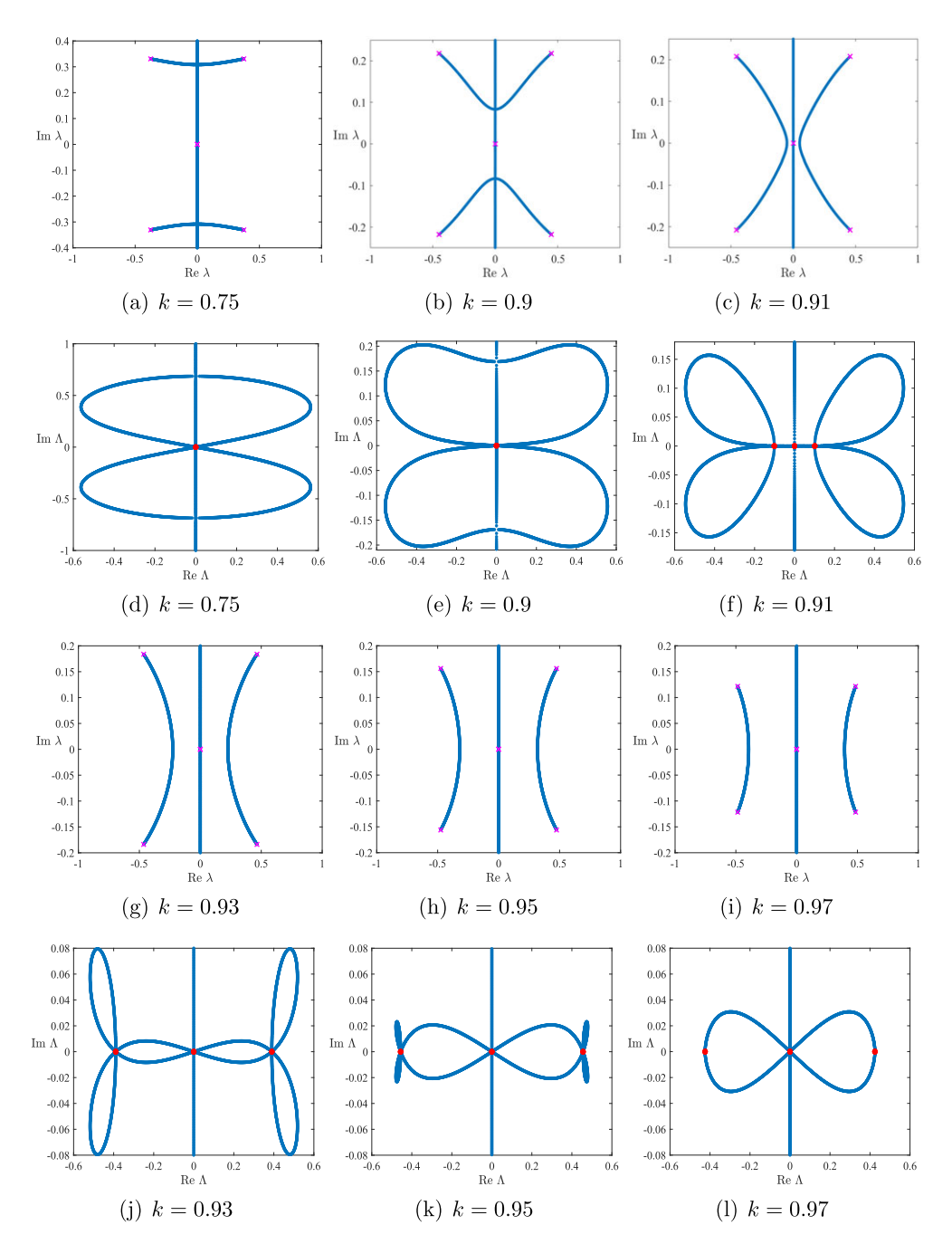


Figure 1. The Lax and stability spectra for the cnoidal wave (1.5) with different values of k. (a)—(c) and (g)—(i): Lax spectrum in λ -plane. (d)—(f) and (j)—(l): stability spectrum in Λ -plane.

The main phenomenon of the transformation of figure-8 to figure- ∞ is shown in figure 1 for the cnoidal wave (1.5) with different values of $k \in (0,1)$. As k crosses $k_* \approx 0.909$, the co-periodic instability arises (the corresponding eigenvalues are shown by red dots on panels (f) and (j)–(l)). This leads to the transformation of the figure-8 (panels (d) and (e)) into a propeller (panel (f)), which becomes a complicated figure with two loops extended along the horizontal direction and four loops extended in the vertical direction (panels (j) and (k)). Finally, the four loops disappear and the figure- ∞ is formed (panel (l)). The point $k=k_*$ corresponds to the marginal case when the

two bands of the Lax spectrum cross at the origin, separating their crossing at the pure imaginary axis for $k < k_*$ (panels (a) and (b)) and at the real axis for $k > k_*$ (panels (c) and (g)–(i)). Four endpoints of the two complex bands of the Lax spectrum are shown by the magenta crosses, these are roots of the characteristic polynomial for the periodic travelling waves, see equation (3.3).

Our analytical study and numerical computations of the spectral stability of the periodic travelling waves of the mKdV equation (1.1) rely on a relation between squared eigenfunctions satisfying the Lax pair and eigenfunctions of the spectral stability problem, see equation (3.5). The method of squared eigenfunctions was explored in a similar context of stability of periodic travelling waves in various integrable models in [32–35]. The spectral stability problem can be solved due to separation of variables and this has been explored for integrable models in [36–39], see also [40,41] for the cases where the spectral stability of periodic travelling waves cannot be studied by separation of variables.

It is interesting to emphasize that the Lax spectrum for the cnoidal wave (1.5) of the focusing mKdV equation (1.1) is identical to that of the cnoidal wave solution of the focusing NLS equation [33,38]. The spectral stability spectrum is, however, very different since the stability spectrum of the cnoidal waves in the focusing NLS equation only features the figure-8 instability [33,38]. Although transformations of the instability bands for Stokes waves in Euler's equations are more complicated than the one in figure 1, see [1,2], the main transformation of figure-8 into figure- ∞ due to the co-periodic instability is well captured by the wave model of the focusing mKdV equation.

The paper is organized as follows. Section 2 presents the waveforms for the periodic travelling waves of the mKdV equation (1.1). Section 3 characterizes the periodic travelling waves by using the Lax pair and gives a relation between the squared eigenfunctions of the Lax pair and the eigenfunctions of the linearized mKdV equation. Section 4 describes the analytical results on the location of the Lax and stability spectra for the two waveforms of the periodic travelling waves. Section 5 contains outcomes of the numerical computations based on a robust numerical algorithm for the approximation of the Lax spectrum. Section 6 gives a summary of our findings.

2. Waveforms for the periodic travelling waves

Integrating the second-order equation (1.3), we obtain the first-order invariant

$$(U')^2 + Q(U) = d, (2.1)$$

where $Q(U) := U^4 - cU^2 - 2bU$ and d is a constant. Two particular waveforms generalizing the dnoidal and cnoidal waves (equations (1.4) and (1.5)) are given in terms of the four roots $\{u_1, u_2, u_3, u_4\}$ of Q(u) = d. The four roots satisfy the relations

$$u_{1} + u_{2} + u_{3} + u_{4} = 0,$$

$$u_{1}u_{2} + u_{1}u_{3} + u_{1}u_{4} + u_{2}u_{3} + u_{2}u_{4} + u_{3}u_{4} = -c,$$

$$u_{1}u_{2}u_{3} + u_{1}u_{2}u_{4} + u_{1}u_{3}u_{4} + u_{2}u_{3}u_{4} = 2b,$$

$$u_{1}u_{2}u_{3}u_{4} = -d,$$

$$(2.2)$$

which follow by expanding

$$Q(u) - d = (u - u_1)(u - u_2)(u - u_3)(u - u_4) = u^4 - cu^2 - 2bu - d.$$
(2.3)

The following proposition states the two waveforms for the periodic travelling waves, see also [13].

Proposition 2.1. If the roots $\{u_1, u_2, u_3.u_4\}$ are real and ordered as $u_4 \le u_3 \le u_2 \le u_1$, then the first-order invariant (2.1) is satisfied by

$$U(x) = u_4 + \frac{(u_1 - u_4)(u_2 - u_4)}{(u_2 - u_4) + (u_1 - u_2)\operatorname{sn}^2(\nu x, k)}$$
(2.4)

where

$$v = \frac{1}{2}\sqrt{(u_1 - u_3)(u_2 - u_4)} \quad \text{and} \quad k = \frac{\sqrt{(u_1 - u_2)(u_3 - u_4)}}{\sqrt{(u_1 - u_3)(u_2 - u_4)}}.$$
 (2.5)

If $\{u_1, u_2\}$ are real and $\{u_3.u_4\}$ are complex-conjugate such that $u_2 \le u_1$ and $u_3 = \bar{u}_4 = \gamma + i\eta$ with $\eta > 0$, then the first-order invariant (2.1) is satisfied by

$$U(x) = u_2 + \frac{(u_1 - u_2)(1 - \operatorname{cn}(\mu x, k))}{(\delta + 1) + (\delta - 1)\operatorname{cn}(\mu x, k)},$$
(2.6)

where

$$\delta = \frac{\sqrt{(u_1 - \gamma)^2 + \eta^2}}{\sqrt{(u_2 - \gamma)^2 + \eta^2}},$$

$$\mu = \sqrt[4]{[(u_1 - \gamma)^2 + \eta^2][(u_2 - \gamma)^2 + \eta^2]},$$

$$2k^2 = 1 - \frac{(u_1 - \gamma)(u_2 - \gamma) + \eta^2}{\sqrt{[(u_1 - \gamma)^2 + \eta^2][(u_2 - \gamma)^2 + \eta^2]}}.$$
(2.7)

Proof. We rewrite equations (2.1) and (2.3) in the form

$$(U')^2 + (U - u_1)(U - u_2)(U - u_3)(U - u_4) = 0.$$

To verify equations (2.4) and (2.5) for $u_4 \le u_3 \le u_2 \le u_1$, we substitute

$$U(x) = u_4 + \frac{(u_1 - u_4)(u_2 - u_4)}{V(x)}$$

and obtain

$$(V')^{2} + [(u_{1} - u_{4}) - V][(u_{2} - u_{4}) - V][(u_{1} - u_{4})(u_{2} - u_{4}) - (u_{3} - u_{4})V] = 0.$$

After substituting $V(x) = (u_2 - u_4) + (u_1 - u_2)W(x)$, we obtain

$$(W')^{2} = W(1 - W)[(u_{1} - u_{3})(u_{2} - u_{4}) - (u_{1} - u_{2})(u_{3} - u_{4})W].$$
(2.8)

The elliptic function $W(x) = \operatorname{sn}^2(\nu x, k)$ satisfies equation (2.8) if ν and k are defined by equation (2.5).

To verify equations (2.6) and (2.7) for $u_2 \le u_1$ and $u_3 = \bar{u}_4 = \gamma + i\eta$ with $\eta > 0$, we rewrite equations (2.1) and (2.3) in the form

$$(U')^{2} + (U - u_{1})(U - u_{2})[(U - \gamma)^{2} + \eta^{2}] = 0.$$

Substituting

$$U(x) = u_1 + \frac{(u_2 - u_1)}{V(x)}$$

yields

$$(V')^{2} + (1 - V)[(u_{1} - \gamma)V + u_{2} - u_{1} + \eta^{2}V^{2}] = 0.$$
(2.9)

The elliptic function

$$V(x) = 1 + \delta \frac{1 + \operatorname{cn}(\mu x, k)}{1 - \operatorname{cn}(\mu x, k)}$$

satisfies equation (2.9) if δ , ν and k are defined by equation (2.7).

Remark 2.2. For periodic solution (2.4), exchanging $u_1 \leftrightarrow u_3$ and $u_2 \leftrightarrow u_4$ yields another periodic solution:

$$U(x) = u_2 + \frac{(u_2 - u_3)(u_2 - u_4)}{(u_4 - u_2) + (u_3 - u_4)\operatorname{sn}^2(vx; k)}$$
(2.10)

with the same definition of ν and k.

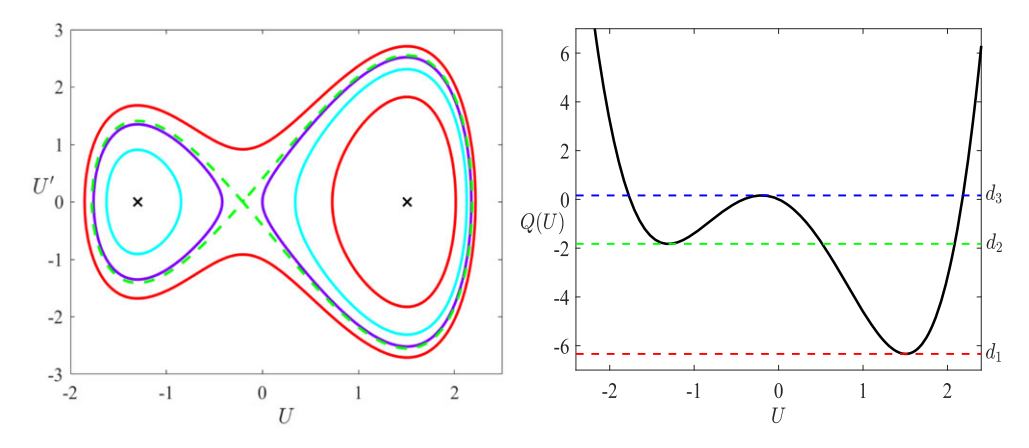


Figure 2. (a) Phase portrait in the phase plane (U, U') for b = 0.8 and c = 4. (b) Levels of d at the plot of Q(U).

Remark 2.3. The periodic solutions U(x) in the form of equations (2.4) and (2.10) are located in the intervals $[u_2, u_1]$ and $[u_4, u_3]$, respectively. In both cases, they have the period $L = 2K(k)v^{-1}$, where K(k) is the complete elliptic integral of the first type. The periodic solution U(x) in the form of equation (2.6) is located in the interval $[u_2, u_1]$ and has the period $L = 4K(k)\mu^{-1}$.

To illustrate the two waveforms in proposition 2.1, we plot the level curves of

$$\mathcal{H}(U, U') = (U')^2 + Q(U)$$

on the phase plane $(U, U') \in \mathbb{R}^2$. Figure 2a shows a typical phase portrait in the case c > 0 and $b \in (-\sqrt{2}c^3/3\sqrt{3}, \sqrt{2}c^3/3\sqrt{3})$, where the saddle point is squeezed between two centre points shown by black crosses. The level curves on the phase plane (U, U') correspond to the region of U, where $Q(U) \le d$, shown in figure 2b.

For $d \in (d_1, d_2)$ and $d \in (d_3, \infty)$, only two real roots of Q(U) = d exist and the solution waveform is given by equation (2.6). For $d \in (d_2, d_3)$, four real roots of Q(U) = d exist and the solution waveforms are given by equations (2.4) and (2.10). In the limiting cases, the solution waveforms degenerate as follows.

- If $d = d_1$, then $u_1 = u_2$ in equation (2.6) and we have the constant solution $U(x) = u_1$;
- If $d = d_2$, then $u_3 = u_4$ in equation (2.4) and we have the trigonometric waveform for the periodic solution:

$$U(x) = u_3 + \frac{(u_1 - u_3)(u_2 - u_3)}{(u_2 - u_3) + (u_1 - u_2)\sin^2(v_3)}$$
 and $v = \frac{1}{2}\sqrt{(u_1 - u_3)(u_2 - u_3)}$.

In addition, we have the constant solution $U(x) = u_3$ from equation (2.10); and

— If $d = d_3$, then either $u_2 = u_3$ in equation (2.4) or $\eta = 0$ and $u_2 < \gamma < u_1$ in equation (2.6). The two cases give two hyperbolic waveforms for the solitary wave solutions:

$$U(x) = u_4 + \frac{(u_1 - u_4)(u_2 - u_4)}{(u_2 - u_4) + (u_1 - u_2)\tanh^2(v_1)}, \quad v = \frac{1}{2}\sqrt{(u_1 - u_2)(u_2 - u_4)}$$

and

$$U(x) = u_4 + \frac{(u_1 - u_4)(u_2 - u_4)(\cosh(2\nu x) - 1)}{(u_1 - u_4)\cosh(2\nu x) + (u_1 - 2u_2 + u_4)}$$
$$= u_4 + \frac{(u_1 - u_4)(u_2 - u_4)\tanh^2(\nu x)}{(u_1 - u_2) + (u_2 - u_4)\tanh^2(\nu x)},$$

where we have relabelled $u_2 \rightarrow u_4$ and $\gamma \rightarrow u_2 = u_3$ in the second solution compared to equation (2.6) and transformed it with $\mu = 2\nu$ to the form similar to the first solution. In addition, we have the constant solution $U(x) = u_2$ from equation (2.10).

3. Lax spectrum for the periodic travelling waves

The mKdV equation (1.1) is a compatibility condition of the following system of the linear equations [42] for $\psi \in \mathbb{C}^2$:

$$\psi_{x} = L(u, \lambda)\psi,
\psi_{t} = M(u, \lambda)\psi,$$
(3.1)

where

$$L(u,\lambda) = \left(\begin{array}{cc} \lambda & u \\ -u & -\lambda \end{array}\right)$$

and

$$M(u,\lambda) = \begin{pmatrix} -4\lambda^3 - 2\lambda u^2 & -4\lambda^2 u - 2\lambda u_x - 2u^3 - u_{xx} \\ 4\lambda^2 u - 2\lambda u_x + 2u^3 + u_{xx} & 4\lambda^3 + 2\lambda u^2 \end{pmatrix}.$$

Solutions of the linear equations (3.1) for the travelling waves of the mKdV equation (1.1) are related to solutions of the linearized mKdV equation at the travelling waves. These relations are well known (e.g. [14]) and are reproduced here for the sake of transparency.

Let u(x,t) = U(x-ct) be the travelling wave solution of the mKdV equation (1.1). Then the linear system (3.1) enjoys the separation of variables in the form $\psi(x,t) = \Psi(x-ct)e^{\Omega t}$, with $\Psi \in \mathbb{C}^2$ and $\Omega \in \mathbb{C}$ found from the linear system

$$\Psi' = L(U, \lambda)\Psi,$$

$$\Omega\Psi = [M(U, \lambda) + cL(U, \lambda)]\Psi.$$
(3.2)

The following proposition gives the admissible values of Ω .

Proposition 3.1. The admissible values of Ω are defined by the characteristic polynomial

$$P(\lambda) = 16\lambda^6 - 8c\lambda^4 + (c^2 + 4d)\lambda^2 - b^2$$
(3.3)

as $\Omega = \pm \sqrt{P(\lambda)}$.

Proof. The second equation in system (3.2) shows that Ω is an eigenvalue of the following matrix

$$A:=\left(\begin{array}{cc} -4\lambda^3-2\lambda U^2+c\lambda & -(4\lambda^2 U+2U^3+U''-cU+2\lambda U') \\ 4\lambda^2 U+2U^3+U''-cU-2\lambda U' & 4\lambda^3+2\lambda U^2-c\lambda \end{array}\right).$$

Since the trace of *A* is zero, $\Omega^2 = P(\lambda) := \det(A)$, which is expanded in powers of λ as follows:

$$P(\lambda) = 16\lambda^6 - 8c\lambda^4 - (12U^4 + 8UU'' - 4cU^2 - 4(U')^2 - c^2)\lambda^2 - (2U^3 + U'' - cU)^2.$$

By using equations (1.3) and (2.1), we rewrite $P(\lambda)$ in the form (3.3).

We define the Lax spectrum of the periodic travelling waves as the set of admissible values of λ in the spectral problem $\Psi' = L(U, \lambda)\Psi$, for which $\Psi \in L^{\infty}(\mathbb{R}, \mathbb{C}^2)$. By Floquet theorem, if U(x + L) = U(x) is L-periodic, then the bounded eigenfunction Ψ is quasi-periodic as $\Psi(x + L) = \Psi(x)$ e^{i μL} with $\mu \in [-\pi/L, \pi/L]$ for the values of λ defined in the continuous bands of the Lax spectrum.

To relate the Lax spectrum with the stability spectrum, we define the linearization of the mKdV equation (1.1) at the periodic travelling waves with the profile U. By using $u(x,t) = U(x-ct) + u(x-ct)e^{\Lambda t}$ and linearizing at u, we obtain the spectral stability problem in the form

$$\Lambda u + u''' + 6(U^2 u)' - c u' = 0. \tag{3.4}$$

The stability spectrum of the periodic travelling waves is defined as the set of admissible values of Λ in the spectral stability problem (3.4), for which $\mathfrak{u} \in L^{\infty}(\mathbb{R}, \mathbb{C})$. By the same Floquet theorem, if U(x+L)=U(x) is L-periodic, then the bounded eigenfunction \mathfrak{u} is quasi-periodic as $\mathfrak{u}(x+L)=\mathfrak{u}(x)$ e^{i θ L} with $\theta \in [-\pi/L, \pi/L]$ for the values of Λ defined in the continuous bands of the stability

spectrum. The bands of Λ in the stability spectrum are related to the bands of λ in the Lax spectrum due to the squared eigenfunction relation [14].

The following proposition gives the relation between eigenfunctions of the spectral stability problem (3.4) and the squared eigenfunctions of the linear system (3.2).

Proposition 3.2. Let $\Sigma \subset \mathbb{C}$ be the Lax spectrum and $\Psi = (p,q)^T \in L^{\infty}(\mathbb{R},\mathbb{C}^2)$ be the eigenfunction of the linear system (3.2) for an admissible value of $\lambda \in \Sigma$. Then, $\mathfrak{u} := p^2 - q^2 \in L^{\infty}(\mathbb{R},\mathbb{C})$ is the eigenfunction of the spectral stability problem (3.4) with

$$\Lambda = 2\Omega = \pm 2\sqrt{P(\lambda)}. (3.5)$$

Proof. Given that $\Psi = (p, q)^T$, we rewrite $\Psi' = L(U, \lambda)\Psi$ into

$$p' = \lambda p + Uq,$$

$$q' = -Up - \lambda q,$$

from which we obtain

$$\begin{cases} p'' = \lambda p' + U'q + Uq' \\ = \lambda^2 p + U'q - U^2 p, \\ q'' = -U'P - Up' - \lambda q' \\ = \lambda^2 q - U^2 q - U'p \end{cases}$$

and

$$\begin{cases} p''' = \lambda^2 p' + U''q + U'q' - 2UU'p - U^2 p' \\ = \lambda^3 p + \lambda^2 Uq + U''q - 3UU'p - \lambda U'q - \lambda U^2 p - U^3 q, \\ q''' = \lambda^2 q' - U''p - U'p' - 2UU'q - U^2 q' \\ = -\lambda^3 q - \lambda^2 Up - U''p - 3UU'q - \lambda U'p + \lambda U^2 q + U^3 p. \end{cases}$$

This yields with explicit computations:

$$(p^2)''' = 2pp''' + 6p'p''$$

$$= 8\lambda^3 p^2 + 8\lambda^2 Upq + 4\lambda U'pq - 8\lambda U^2 p^2 - 8U^3 pq + 6UU'q^2 - 6UU'p^2 + 2U''pq$$

and

$$(q^2)''' = 2pp''' + 6p'p''$$

$$= -8\lambda^3 q^2 - 8\lambda^2 Upq + 4\lambda U'pq + 8\lambda U^2 q^2 + 8U^3 pq - 6UU'q^2 + 6UU'p^2 - 2U''pq.$$

Combining with the second equation of system (3.2), we obtain

$$(p^2)''' + 12UU'p^2 + 6U^2(p^2)' - c(p^2)'$$

$$= 8\lambda^3 p^2 + 8\lambda^2 Upq + 4\lambda U'pq + 4\lambda U^2 p^2 + 4U^3 pq + 2U''pq + 6UU'q^2 + 6UU'p^2$$

$$= -2\Omega p^2 + 6UU'(p^2 + q^2)$$

and

$$\begin{split} &(q^2)''' + 12UU'q^2 + 6U^2(q^2)' - c(q^2)' \\ &= -8\lambda^3 q^2 - 8\lambda^2 Upq + 4\lambda U'pq - 4\lambda U^2q^2 - 4U^3pq - 2U''pq + 6UU'q^2 + 6UU'p^2 \\ &= -2\Omega q^2 + 6UU'(p^2 + q^2), \end{split}$$

which verify that

$$\mathfrak{u}''' + 12UU'\mathfrak{u} + 6U^2\mathfrak{u}' - c\mathfrak{u}' = -2\Omega\mathfrak{u},$$

for $u := p^2 - q^2$. This equation is equivalent to (3.4) with $\Lambda = 2\Omega$, whereas the relation $\Omega = \pm \sqrt{P(\lambda)}$ is established in proposition 3.1.

4. Lax and stability spectra: analytical results

Although the exact location of the Lax spectrum for the periodic travelling waves is not known, the symmetry of the Lax spectrum with respect to reflection about $\lambda = 0$ and about the real axis follow the symmetry of $L(u, \lambda)$ in the linear system (3.1). The following proposition states these properties of the Lax spectrum.

Proposition 4.1. Let $\lambda \in \mathbb{C}$ be an eigenvalue of the spectral problem $\psi_x = L(u, \lambda)\psi$ with the eigenfunction $\psi = (p, q)^T \in L^{\infty}(\mathbb{R}, \mathbb{C}^2)$. Then, $-\lambda$ is also an eigenvalue with the eigenfunction $\psi = (q, -p)^T \in L^{\infty}(\mathbb{R}, \mathbb{C}^2)$. Moreover, if $\lambda \notin \mathbb{R}$, then $\bar{\lambda}$ is also an eigenvalue with the eigenfunction $\psi = (\bar{p}, \bar{q})^T \in L^{\infty}(\mathbb{R}, \mathbb{C}^2)$.

Proof. We rewrite $\psi_x = L(u, \lambda)\psi$ in the form:

$$p_x = \lambda p + uq,$$

$$q_x = -up - \lambda q.$$

This implies

$$q_x = (-\lambda)q + u(-p),$$

$$-p_x = -\lambda p - uq,$$

so that $\psi := (q, -p)^T$ is also a solution of $\psi_x = L(u, \lambda)\psi$ with eigenvalue $-\lambda$. Furthermore, taking the complex-conjugate transform yields

$$\begin{bmatrix}
 \bar{p}_x = \bar{\lambda}\bar{p} + \bar{u}\bar{q}, \\
 \bar{q}_x = -\bar{u}\bar{p} - \bar{\lambda}\bar{q}.
 \end{bmatrix}$$

Since $u = \bar{u}$ and $\lambda \neq \bar{\lambda}$, then $\psi := (\bar{p}, \bar{q})^T$ is also a solution of $\psi_x = L(u, \lambda)\psi$ with eigenvalue $\bar{\lambda}$.

Roots of the characteristic polynomial $P(\lambda)$ in equation (3.3) can be enumerated as $\{\pm\lambda_1, \pm\lambda_2, \pm\lambda_3\}$. It was found in [43–46] that roots of $P(\lambda)$ are related to roots $\{u_1, u_2, u_3.u_4\}$ of Q(u) = d in equation (2.1). These relations were verified for the mKdV equation in [13] with a direct proof, hence we state the relations without further details:

$$\lambda_1 = \frac{1}{2}(u_1 + u_2), \quad \lambda_2 = \frac{1}{2}(u_1 + u_3), \quad \lambda_3 = \frac{1}{2}(u_2 + u_3).$$
 (4.1)

It was shown in [13] that spectral bands of the Lax spectrum for the periodic travelling waves outside $i\mathbb{R}$ are connected between the roots $\{\pm\lambda_1, \pm\lambda_2, \pm\lambda_3\}$. In the next two theorems, we derive the stability criterion for the waveform (2.4) and the instability criterion for the waveform (2.6) in the spectral stability problem (3.4). It relies on the location of the spectral bands between the roots of $P(\lambda)$ in addition to the spectral bands on $i\mathbb{R}$, which is assumed here and verified numerically in §5, as well as the squared eigenfunction relation of proposition 3.2.

Theorem 4.2. For the waveform (2.4) of proposition 2.1, assume that the Lax spectrum is located on

$$i\mathbb{R} \cup [-\lambda_1, -\lambda_2] \cup [-|\lambda_3|, |\lambda_3|] \cup [\lambda_2, \lambda_1]. \tag{4.2}$$

Then the stability spectrum is $i\mathbb{R}$.

Proof. For the waveform (2.4) of proposition 2.1, the roots $\{u_1, u_2, u_3. u_4\}$ of Q(u) = d are real and ordered as $u_4 \le u_3 \le u_2 \le u_1$. By (4.1), the roots $\{\pm \lambda_1, \pm \lambda_2, \pm \lambda_3\}$ of $P(\lambda)$ are real and ordered as $\lambda_3 \le \lambda_2 \le \lambda_1$. Moreover, due to the first relation in (2.2), we have $u_2 + u_3 = -u_1 - u_4$. If $u_2 + u_3 < 0$, then $|u_2 + u_3| = u_1 + u_4 \le u_1 + u_3$, which proves that $|\lambda_3| \le \lambda_2$ even if $\lambda_3 < 0$. Hence, we have $0 \le |\lambda_3| \le \lambda_2 \le \lambda_1$.

For $\lambda \in i\mathbb{R}$ in the Lax spectrum (4.2), we rewrite the polynomial $P(\lambda)$ in the form:

$$\begin{split} P(\lambda) &= 16(\lambda^2 - \lambda_1^2)(\lambda^2 - \lambda_2^2)(\lambda^2 - \lambda_3^2) \\ &= -16(|\lambda|^2 + \lambda_1^2)(|\lambda|^2 + \lambda_2^2)(|\lambda|^2 + \lambda_3^2). \end{split}$$

Since $P(\lambda) < 0$, we have $\Lambda = \pm 2\sqrt{P(\lambda)} \in i\mathbb{R}$ by (3.5). Moreover, $\lim_{|\lambda| \to \infty} P(\lambda) = -\infty$ and $\lim_{\lambda \to 0} P(\lambda) = -16\lambda_1^2 \lambda_2^2 \lambda_3^2$ so that

$$(-\infty, -8\lambda_1\lambda_2|\lambda_3|] \cup [8\lambda_1\lambda_2|\lambda_3|, \infty)i$$

belongs to the stability spectrum.

For $\lambda \in [-\lambda_1, -\lambda_2] \cup [-|\lambda_3|, |\lambda_3|] \cup [\lambda_2, \lambda_1]$ in the Lax spectrum (4.2), we have $P(\lambda) \leq 0$ so that $\Lambda = \pm 2\sqrt{P(\lambda)} \in i\mathbb{R}$ by (3.5). Moreover, $\lim_{|\lambda| \to |\lambda_3|} P(\lambda) = 0$ so that

$$[-8\lambda_1\lambda_2|\lambda_3|, 8\lambda_1\lambda_2|\lambda_3|]i$$

also belongs to the stability spectrum. Hence, the image of $\Lambda = \pm 2\sqrt{P(\lambda)}$ covers all $i\mathbb{R}$.

Remark 4.3. The parts of the Lax spectrum (4.2) for $\lambda \in [-\lambda_1, -\lambda_2] \cup [\lambda_2, \lambda_1]$ cover a subset of $i\mathbb{R}$ for the second time. Regardless, the periodic travelling wave with the waveform (2.4) is classified as spectrally stable.

Theorem 4.4. For the waveform (2.6) of proposition 2.1, assume that the Lax spectrum is located on

$$i\mathbb{R} \cup [-|\lambda_1|, |\lambda_1|] \cup \Sigma_+ \cup \Sigma_-,$$
 (4.3)

where Σ_+ is the spectral band connecting two complex roots in the set $\{\pm \lambda_2, \pm \lambda_3\}$ and Σ_- is the reflection of Σ_+ about $\lambda = 0$. Then the stability spectrum is the union of $i\mathbb{R}$ and the spectral bands which are not contained in $i\mathbb{R}$ and are symmetric about $\Lambda = 0$.

Proof. For the waveform (2.6) of proposition 2.1, the roots $\{u_1, u_2\}$ of Q(u) = d are real and ordered as $u_2 \le u_1$, whereas the roots $\{u_3, u_4\}$ are complex-conjugate with $u_3 = \bar{u}_4 = \gamma + i\eta$ and $\eta > 0$. By (4.1), the roots $\{\pm \lambda_1\}$ of $P(\lambda)$ are real, whereas the roots $\{\pm \lambda_2, \pm \lambda_3\}$ represent a complex-conjugate quadruplet since

$$\lambda_3 = \frac{1}{2}(u_2 + u_3) = -\frac{1}{2}(u_1 + u_4) = -\frac{1}{2}(u_1 + \bar{u}_3) = -\bar{\lambda}_2,$$

due to the first relation in (2.2). Since $\lambda_2 = -\bar{\lambda}_3$, we can rewrite $P(\lambda)$ in the form:

$$P(\lambda) = 16(\lambda^2 - \lambda_1^2)[(\lambda^2 - \text{Re}(\lambda_2^2))^2 + (\text{Im}(\lambda_2^2))^2].$$

For $\lambda \in i\mathbb{R}$ in the Lax spectrum (4.3), we have $P(\lambda) < 0$, and since $\lim_{|\lambda| \to \infty} P(\lambda) = -\infty$ and $\lim_{\lambda \to 0} P(\lambda) = -16\lambda_1^2 \lambda_2^2 \lambda_3^2$, we have by $\Lambda = \pm 2\sqrt{P(\lambda)}$ that

$$(-\infty, -8|\lambda_1||\lambda_2|^2] \cup [8|\lambda_1||\lambda_2|^2, \infty)i$$

belongs to the stability spectrum.

For $\lambda \in [-|\lambda_1|, |\lambda_1|]$ in the Lax spectrum (4.3), we have $P(\lambda) \le 0$ and since $\lim_{|\lambda| \to |\lambda_1|} P(\lambda) = 0$, we have by $\Lambda = \pm 2\sqrt{P(\lambda)}$ that

$$[-8|\lambda_1||\lambda_2|^2, 8|\lambda_1||\lambda_2|^2]i$$

also belongs to the stability spectrum. Hence, the image of $\Lambda = \pm 2\sqrt{P(\lambda)}$ covers all $i\mathbb{R}$.

It remains to prove that the image of $\Lambda=\pm 2\sqrt{P(\lambda)}$ for $\lambda\in \Sigma_+$ in the Lax spectrum (4.3) is not contained in $i\mathbb{R}$. Since Σ_- is a reflection of Σ_+ about $\lambda=0$ and $\Lambda=0$ if $\lambda=\pm \lambda_2$ or $\lambda=\pm \lambda_3$, the image of $\Lambda=\pm 2\sqrt{P(\lambda)}$ for $\lambda\in \Sigma_-$ is a reflection of the image of $\Lambda=\pm 2\sqrt{P(\lambda)}$ for $\lambda\in \Sigma_+$ about $\Lambda=0$, so that the spectral bands are not contained in $i\mathbb{R}$ and are symmetric about $\Lambda=0$.

Let $\lambda \in \Sigma_+$. Owing to symmetries between $\{\pm \lambda_2, \pm \bar{\lambda}_2\}$, we may have only four possibilities, for each we prove that there exists $\lambda \in \Sigma_+$ such that $\Lambda = \pm 2\sqrt{P(\lambda)} \notin i\mathbb{R}$.

— Σ_+ connects λ_2 and $\bar{\lambda}_2$ and crosses \mathbb{R} outside the segment $[0, |\lambda_1|]$. For $\lambda_0 \in \Sigma_+ \cap \mathbb{R}$, $P(\lambda_0) > 0$ so that $\Lambda = \pm 2\sqrt{P(\lambda_0)} \in \mathbb{R}$;

- Σ_+ connects λ_2 and $\bar{\lambda}_2$ and crosses \mathbb{R} inside the segment $(0, |\lambda_1|]$. Σ_+ and \mathbb{R} intersect perpendicularly at $\lambda_0 \in \Sigma_+ \cap \mathbb{R}$ due to the symmetry of Lax spectrum in proposition 4.1 and $P(\lambda_0) \leq 0$. Hence, there is $\lambda \in \Sigma_+$ such that $|\lambda \lambda_0|$ is small and $|\text{Re}(\lambda \lambda_0)| \ll |\text{Im}(\lambda)|$. Since $P'(\lambda_0) \in \mathbb{R}$, we have $\text{Re}(P(\lambda)) \leq 0$ and $\text{Im}(P(\lambda)) \neq 0$ for this λ so that $\Lambda = \pm 2\sqrt{P(\lambda)} \notin i\mathbb{R}$;
- Σ_+ connects λ_2 and 0 but does not intersect $(\mathbb{R} \cup i\mathbb{R})\setminus\{0\}$. Since P(0) < 0, P'(0) = 0, and $P''(0) \in \mathbb{R}$, we have $\text{Re}(P(\lambda)) < 0$ and $\text{Im}(P(\lambda)) \neq 0$ for every $\lambda \in \Sigma_+$ with small $|\lambda|$ and $\text{Re}(\lambda)\text{Im}(\lambda) \neq 0$ so that $\Lambda = \pm 2\sqrt{P(\lambda)} \notin i\mathbb{R}$; and
- Σ_+ connects λ_2 and $-\bar{\lambda}_2$ and crosses $i\mathbb{R}$. Σ_+ and $i\mathbb{R}$ intersect perpendicularly at $\lambda_0 \in \Sigma_+ \cap i\mathbb{R}$ due to the symmetry of Lax spectrum in proposition 4.1 and $P(\lambda_0) < 0$. Hence, there is $\lambda \in \Sigma_+$ such that $|\lambda \lambda_0|$ is small and $|\operatorname{Im}(\lambda \lambda_0)| \ll |\operatorname{Re}(\lambda)|$. Since $P'(\lambda_0) \in i\mathbb{R}$, we have $\operatorname{Re}(P(\lambda)) < 0$ and $\operatorname{Im}(P(\lambda)) \neq 0$ for this λ so that $\Lambda = \pm 2\sqrt{P(\lambda)} \notin i\mathbb{R}$.

The list of four possibilities above is complete.

5. Lax and stability spectra: numerical results

We use the Fourier collocation method, see [47, Chapter 2, p.45], to approximate Lax spectrum of $\Psi' = L(U, \lambda)\Psi$ numerically for the travelling waves with the periodic profile U. This numerical method has been used in our previous work [39]. For every λ in the Lax spectrum, the stability spectrum is obtained from $\Lambda = \pm 2\sqrt{P(\lambda)}$ as in equation (3.5). The numerical results verify the assumptions of theorems 4.2 and 4.4 and illustrate their conclusions.

(a) Waveform (2.4)

We take four real roots $\{u_1, u_2, u_3, u_4\}$ of Q(u) = d in the particular setting of $u_1 = 1, u_2 = 0.5, u_3 = 0$, and $u_4 = -u_1 - u_2 - u_3 = -1.5$. The Lax spectrum is shown in figure 3a in agreement with (4.2), where the magenta crosses represent the roots of $P(\lambda)$. The stability spectrum shown in figure 3b is equivalent to $i\mathbb{R}$ in agreement with theorem 4.2.

(b) Waveform (2.6)

We take two real roots of Q(u)=d as $u_1=1$ and $u_2=0.2$ and the two complex-conjugate roots as $u_3=\bar{u}_4=-0.6+0.6i$ so that $u_1+u_2+u_3+u_4=0$. The Lax spectrum is shown in figure 4a in agreement with (4.3). The stability spectrum is shown in figure 4b in agreement with theorem 4.4. The complex bands Σ_{\pm} in (4.3) are connected across $i\mathbb{R}$ in the Lax spectrum so that $\Sigma_{-}=\bar{\Sigma}_{+}$. The stability spectrum is a standard figure-8 instability band.

For a different set of parameter values, the complex bands Σ_{\pm} in (4.3) are connected across \mathbb{R} in the Lax spectrum so that $\Sigma_{-}=-\bar{\Sigma}_{+}$. This is illustrated in figure 5 for the choice of $u_1=1, u_2=-0.2$, and $u_3=\bar{u}_4=-0.4+0.2i$. Nevertheless, the stability spectrum is still a standard figure-8 instability band.

At first glance, readers may get the impression that the cascade of instabilities for the cnoidal wave (1.5) shown in figure 1 is not observed for the periodic waveform (2.6). However, this is just because the two parameter configurations in figures 4 and 5 do not represent a general picture.

To unfold the cascade of instability bifurcations for the periodic waveform (2.6), we parameterize the roots of Q(u) = d with parameters $\kappa \in (0, 1)$ and $\epsilon \in (0, 2\kappa)$ as

$$u_1 = \kappa$$
, $u_2 = -\kappa + \epsilon$, $\gamma = -\frac{\epsilon}{2}$, $\eta = \sqrt{1 - \kappa^2}$.

The periodic waveform (2.6) becomes

$$U(x) = \kappa + \frac{(-2\kappa + \epsilon)(1 - \operatorname{cn}(\mu x; k))}{1 + \delta + (\delta - 1)\operatorname{cn}(\mu x; k)},$$
(5.1)

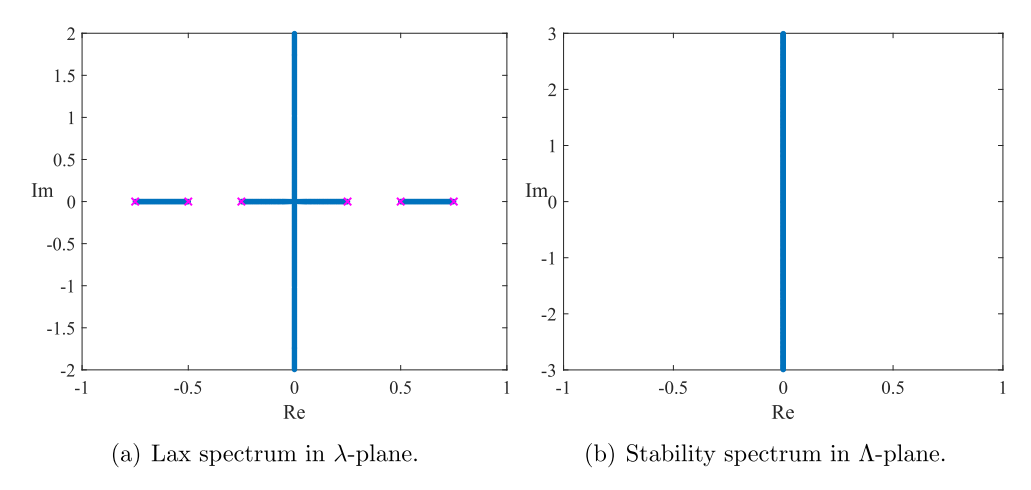


Figure 3. Numerically computed Lax and stability spectra for the periodic solution with the profile (2.4) for $u_1 = 1$, $u_2 = 0.5$, $u_3 = 0$, and $u_4 = -1.5$. (a) Lax spectrum in λ -plane. (b) Stability spectrum in Λ -plane.

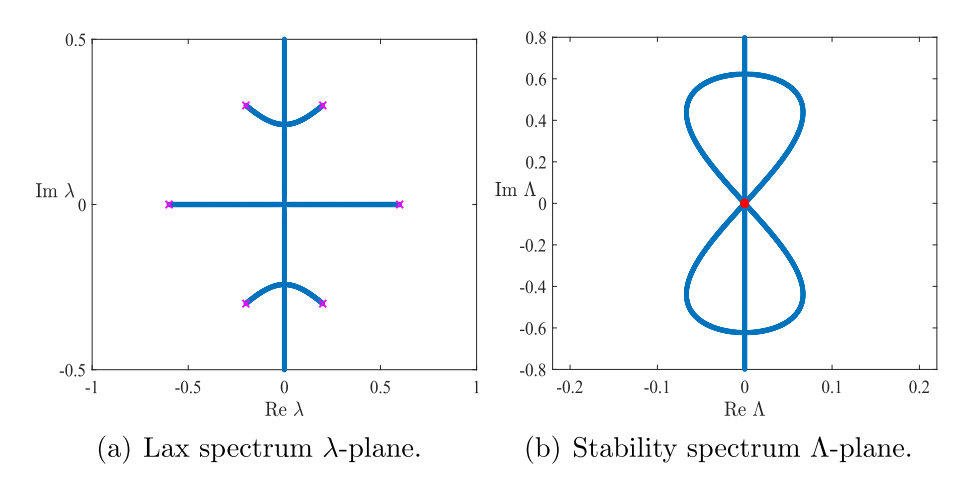


Figure 4. Numerically computed Lax and stability spectra for the periodic solution with the profile (2.6) for $u_1 = 1$, $u_2 = 0.2$, and $u_3 = \bar{u}_4 = -0.6 + 0.6i$. (a) Lax spectrum λ -plane. (b) Stability spectrum Λ -plane.

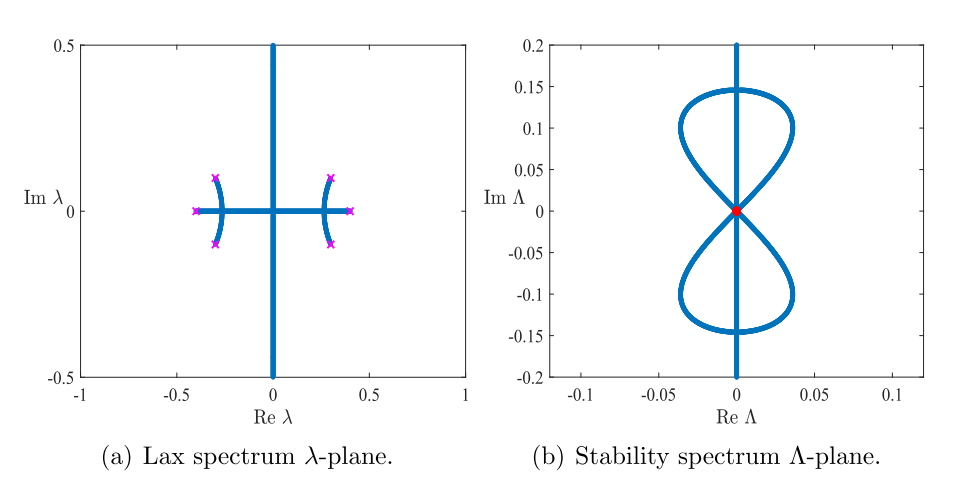


Figure 5. The same as in figure 4 but for $u_1 = 1$, $u_2 = -0.2$, and $u_3 = \bar{u}_4 = -0.4 + 0.2i$. (a) Lax spectrum λ -plane. (b) Stability spectrum Λ -plane.

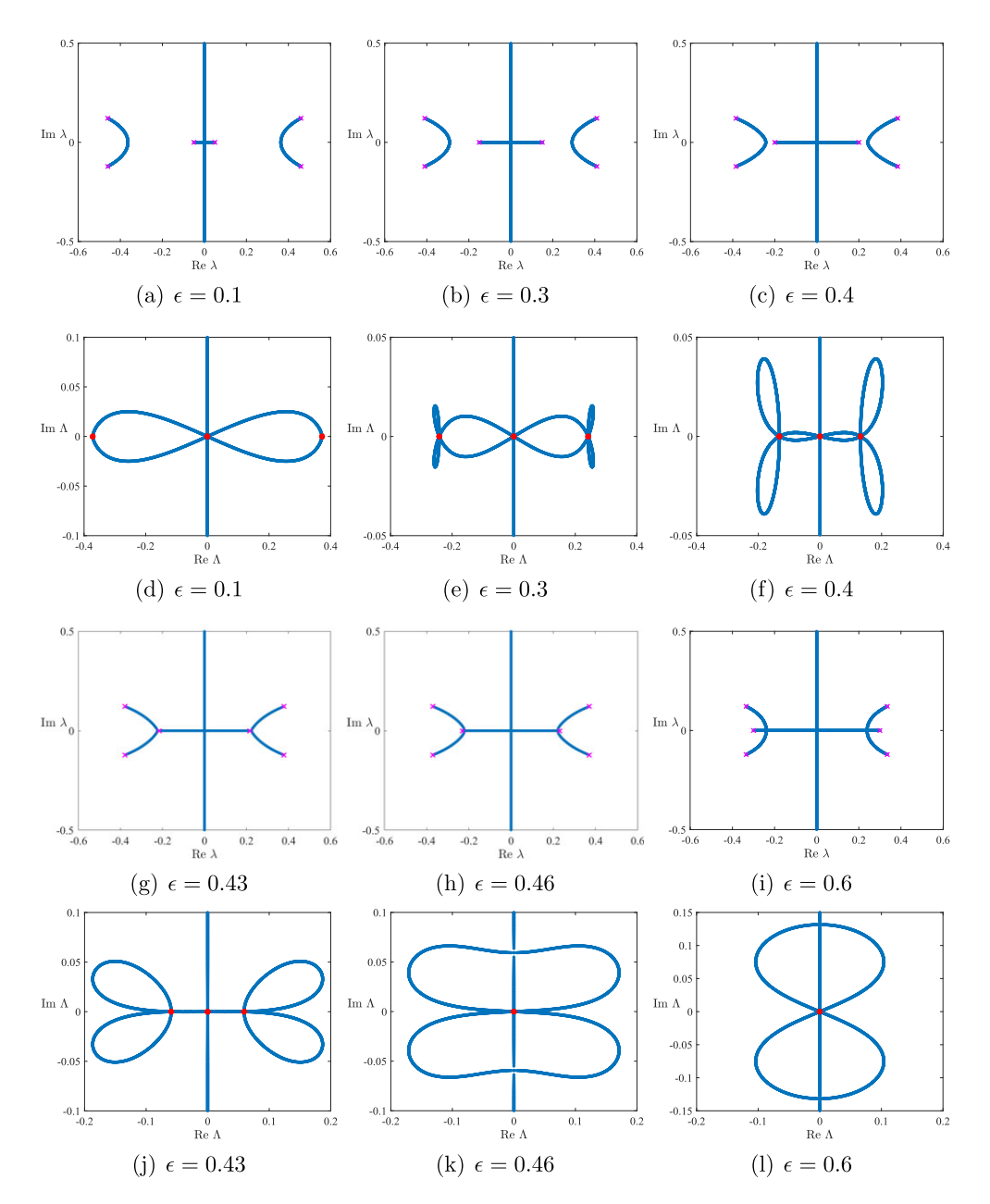


Figure 6. The Lax and stability spectra for periodic waveform (5.1) with $\kappa = 0.97$ and different values of ϵ . (a)—(c) and (g)—(i): Lax spectrum in λ -plane; (d)—(f) and (j)—(l): stability spectrum in Λ -plane.

where

$$\begin{split} \delta &= \frac{\sqrt{\left(\kappa - \frac{3}{2}\epsilon\right)^2 + 1 - \kappa^2}}{\sqrt{\left(\kappa + \frac{\epsilon}{2}\right)^2 + 1 - \kappa^2}}, \\ \mu &= \sqrt[4]{\left[\left(\kappa - \frac{3}{2}\epsilon\right)^2 + 1 - \kappa^2\right] \left[\left(\kappa + \frac{\epsilon}{2}\right)^2 + 1 - \kappa^2\right]} \end{split}$$

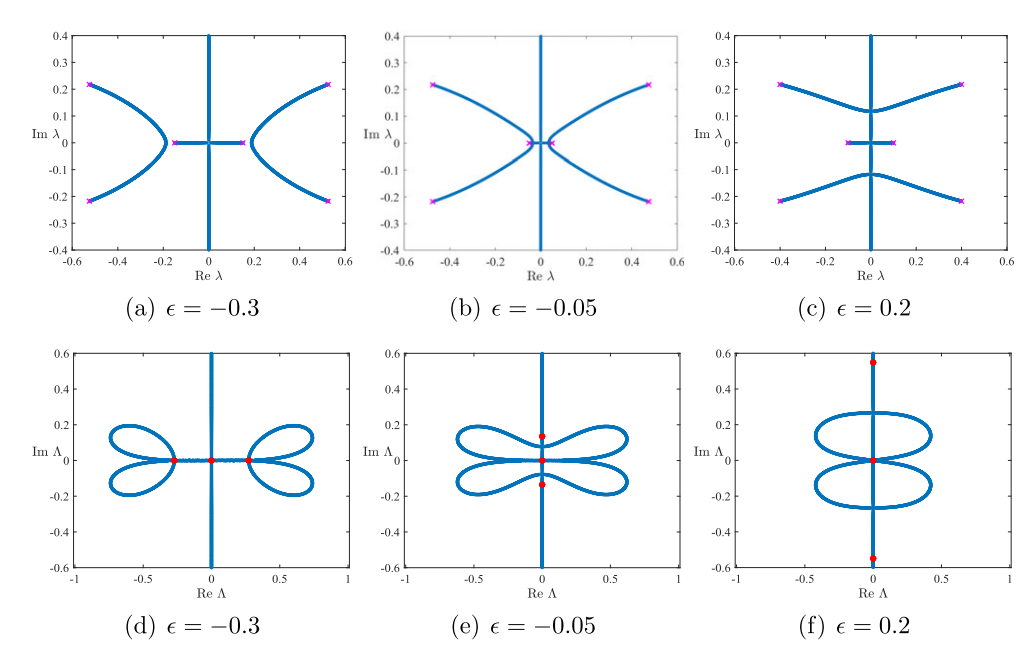


Figure 7. The Lax and stability spectra for periodic waveform (5.1) with $\kappa = 0.9$ and different values of ϵ . (a)–(c): Lax spectrum in λ -plane; (d)–(f): stability spectrum in Λ -plane.

and
$$2k^2 = 1 - \frac{\left(\kappa - \frac{\epsilon}{2}\right)\left(-\kappa + \frac{3}{2}\epsilon\right) + 1 - \kappa^2}{\mu^2}.$$

When $\epsilon = 0$, we have $\delta = 1$, $\mu = 1$, and $k = \kappa$ so that we recover the cnoidal wave with the profile $U(x) = \kappa \operatorname{cn}(x; \kappa)$ as in the periodic solution (1.5).

We fix $\kappa = 0.97$ and compute numerically the Lax and stability spectra for different values of $\epsilon \in (0, 2\kappa)$. The calculated Lax and stability spectra shown in figure 6 turn out to be very similar to those shown on figure 1 for the cnoidal wave (1.5). The only difference from figure 1 is that figure-8 in panel (l) corresponds to the segments Σ_{\pm} of the Lax spectrum in theorem 4.4 crossing the real line in panel (i) and that the line segment $[-|\lambda_1|, |\lambda_1|]$ has a non-zero length. The coperiodic instability (red points on the stability spectrum) arises when the segments Σ_{\pm} of the Lax spectrum touch the endpoints of the line segment $[-|\lambda_1|, |\lambda_1|]$.

If we fix $\kappa=0.9$ and change ϵ to the negative values as well, then the computed Lax and stability spectra shown in figure 7 features a different transformation of the instability bands. The figure-8 instability in panel (f) is related to the segments Σ_{\pm} of the Lax spectrum in theorem 4.4 crossing the imaginary line in panel (c). The co-periodic instability (red points on the stability spectrum) arises again when the segments Σ_{\pm} of the Lax spectrum touch the endpoints of the line segment $[-|\lambda_1|, |\lambda_1|]$. The co-periodic instability is present when the segments Σ_{\pm} intersect the real line outside $[-\lambda_1, \lambda_1]$ and is absent when they intersect the real line inside $[-\lambda_1, \lambda_1]$.

For the cnoidal wave in figure 1, the line segment $[-|\lambda_1|, |\lambda_1|]$ shrinks to the origin and the co-periodic instability arises when the segments Σ_{\pm} of the Lax spectrum touch the origin. Hence, all four cases analysed in the proof of theorem 4.4 do actually occur in the Lax spectrum for the waveform (2.6) with different parameter values.

6. Conclusion

We have studied the spectral stability of the periodic travelling waves in the focusing mKdV equation and showed that the instability bands for the cnoidal periodic waves transform from

figure-8 into figure- ∞ due to the co-periodic instability bifurcation. This transformation is rather generic for other models with periodic travelling waves (Stokes waves) [1,3,11].

The conclusion was obtained by using a relation between squared eigenfunctions of the Lax pair and eigenfunctions of the linearized mKdV equation at the periodic travelling waves. The location of the Lax spectrum remains an open problem, especially for the cnoidal periodic waves. It is expected that the elliptic function theory can be useful to compute it explicitly.

Given universality of the focusing mKdV equation for many applications in fluids, optics and plasmas, the conclusions obtained in this work can be used for the comprehensive study of the modulational instability of the cnoidal periodic waves in the relevant non-integrable models.

Data accessibility. Please see the electronic supplementary material for code. The data are provided in the electronic supplementary material [48].

Declaration of Al use. We have not used AI-assisted technologies in creating this article.

Authors' contributions. S.C.: data curation, investigation, visualization and writing—original draft; D.P.: project administration, supervision, validation and writing—review and editing.

Both authors gave final approval for publication and agreed to be held accountable for the work performed therein.

Conflict of interest declaration. We declare we have no competing interests.

Funding. The work of S. Cui was conducted during PhD studies while visiting McMaster University with the financial support from the China Scholarship Council. The work of D. E. Pelinovsky was supported in part by the National Natural Science Foundation of China (grant no. 12371248).

References

- 1. Deconinck B, Dyachenko SA, Lushnikov PM, Semenova A. 2023 'The dominant instability of near extreme Stokes waves. *Proc. Natl Acad. Sci. USA* **120**, e2308935120. (doi:10.1073/pnas.2308935120)
- 2. Deconinck B, Dyachenko S, Semenova A. 2024 Self-similarity and recurrence in stability spectra of near extreme Stokes waves. *J. Fluid Mech.* **995**, A2. (doi:10.1017/jfm.2024.626)
- 3. Deconinck B, Oliveras K. 2011 The instability of periodic surface gravity waves. *J. Fluid Mech.* **675**, 141–167. (doi:10.1017/S0022112011000073)
- 4. Dyachenko SA, Semenova A. 2023 Quasiperiodic perturbations of Stokes waves: Secondary bifurcations and stability. *J. Comput. Phys.* **492**, 112411. (doi:10.1016/j.jcp.2023.112411)
- 5. Dyachenko SA, Semenova A. 2023 Canonical conformal variables based method for stability of Stokes waves. *Stud. Appl. Math.* **150**, 705–715. (doi:10.1111/sapm.12554)
- 6. Korotkevich AO, Lushnikov PM, Semenova A, Dyachenko SA. 2023 Superharmonic instability of Stokes waves. *Stud. Appl. Math.* **150**, 119–134. (doi:10.1111/sapm.12535)
- 7. Berti M, Maspero A, Ventura P. 2022 Full description of Benjamin-Feir instability of Stokes waves in deep water. *Invent. Math.* 230, 651–711. (doi:10.1007/s00222-022-01130-z)
- 8. Berti M, Maspero A, Ventura P. 2023 Benjamin-Feir instability of Stokes waves in finite depth. *Arch. Ration. Mech. Anal.* **247**, 91. (doi:10.1007/s00205-023-01916-2)
- 9. Berti M, Maspero A, Ventura P. 2024 Stokes waves at the critical depth are modulationally unstable. *Commun. Math. Phys.* **405**, 56. (doi:10.1007/s00220-023-04928-x)
- 10. Creedon RP, Deconinck B. 2023 A high-order asymptotic analysis of the Benjamin–Feir instability spectrum in arbitrary depth. *J. Fluid Mech.* **956**, A29. (doi:10.1017/jfm.2022.1031)
- 11. Carter JD. 2024 Instability of near-extreme solutions to the Whitham equation. *Stud. Appl. Math.* **152**, 903–915. (doi:10.1111/sapm.12668)
- 12. Chen J, Pelinovsky DE. 2018 Rogue periodic waves of the modified KdV equation. *Nonlinearity* **31**, 1955–1980. (doi:10.1088/1361-6544/aaa2da)
- 13. Chen J, Pelinovsky DE. 2019 Periodic travelling waves of the modified KdV equation and rogue waves on the periodic background. *J. Nonlinear Sci.* **29**, 2797–2843. (doi:10.1007/s00332-019-09559-y)
- 14. Deconinck B, Nivala M. 2011 The stability analysis of the periodic traveling wave solutions of the mKdV equation. *Stud. Appl. Math.* **126**, 17–48. (doi:10.1111/j.1467-9590.2010.00496.x)
- 15. El GA, Hoefer MA, Shearer M. 2017 Dispersive and diffusive-dispersive shock waves for nonconvex conservation laws. *SIAM Rev.* **59**, 3–61. (doi:10.1137/15M1015650)

- 16. Girotti M, Grava T, Jenkins R, McLaughlin KT-R, Minakov A. 2023 Soliton versus the gas: Fredholm determinants, analysis, and the rapid oscillations behind the kinetic equation. *Commun. Pure Appl. Math.* **76**, 3233–3299. (doi:10.1002/cpa.22106)
- 17. Ling L, Sun X. 2023 Stability of elliptic function solutions for the focusing modified KdV equation. *Adv. Math.* **435**, 109356. (doi:10.1016/j.aim.2023.109356)
- 18. Ling L, Sun X. 2023 The multi elliptic-breather solutions and their asymptotic analysis for the MKDV equation. *Stud. Appl. Math.* **150**, 135–183. (doi:10.1111/sapm.12536)
- 19. Angulo J. 2007 Non-linear stability of periodic travelling-wave solutions for the Schrödinger and modified Korteweg-de Vries equation. *J. Differ. Equ.* **235**, 1–30. (doi:10.1016/j.jde. 2007.01.003)
- 20. Angulo J, Natali F. 2016 On the instability of periodic waves for dispersive equations. *Differ. Int. Equ.* 29, 837–874. (doi:10.57262/die/1465912606)
- 21. Bronski JC, Johnson MA, Kapitula T. 2011 An index theorem for the stability of periodic travelling waves of Korteweg-de Vries type. *Proc. R. Soc. Edinb. Sect. A* 141, 1141–1173. (doi:10.1017/S0308210510001216)
- 22. Bronski JC, Hur VM, Johnson MA. 2016 Modulational instability in equations of KdV type. In *New Approaches to Nonlinear Waves*, Lecture Notes in Physics, vol. 908, pp. 83–133. Berlin, Germany: Springer.
- 23. Deconinck B, Kapitula T. 2015 On the spectral and orbital stability of spatially periodic stationary solutions of generalized Korteweg-de Vries equations. In *Hamiltonian Partial Differential Equations and Applications*, Fields Institute Communications, vol. 75, pp. 385–322. New York, NY: Springer.
- 24. Le U, Pelinovsky DE. 2022 Periodic waves of the modified KdV equation as minimizers of a new variational problem. *SIAM J. Appl. Dyn. Syst.* 21, 2518–2534. (doi:10.1137/21M1465329)
- 25. Natali F, Le U, Pelinovsky DE. 2022 Periodic waves in the modified fractional Korteweg–de Vries equation. *J. Dyn. Differ. Equ.* **34**, 1601–1640. (doi:10.1007/s10884-021-10000-w)
- 26. Pelinovsky DE. 2014 Spectral stability of nonlinear waves in KdV-type evolution equations. In *Nonlinear Physical Systems: Spectral Analysis, Stability, and Bifurcations* (eds ON Kirillov, DE Pelinovsky), pp. 377–400. Hoboken, NJ: Wiley-ISTE.
- 27. Kenig CE, Ponce G, Vega L. 1993 Well-posedness and scattering results for the generalized Korteweg-de Vries equation via the contraction principle. *Comm. Pure Appl. Math.* **46**, 527–620. (doi:10.1002/cpa.3160460405)
- 28. Colliander J, Keel M, Staffilani G, Takaoka H, Tao T. 2003 Sharp global well-posedness for KdV and modified KdV on ℝ and T. J. Am. Math. Soc. 16, 705–749. (doi:10.1090/S0894-0347-03-00421-1)
- 29. Harrop–Griffiths B, Killip R, Visan M. 2024 Sharp well-posedness for the cubic NLS and mKdV in $H^s(\mathbb{R})$. Forum Math. Pi 12, Paper No. e6.
- 30. Andrade TP, Pastor A. 2019 Orbital stability of one-parameter periodic traveling waves for dispersive equations and applications. *J. Math. Anal. Appl.* 475, 1242–1275. (doi:10.1016/j.jmaa.2019.03.011)
- 31. Pelinovsky DE. 2024 Traveling waves in fractional models. In *Fractional Dispersive Models and Applications: Recent Developments and Future Perspectives* (eds PG Kevrekidis, J Cuevas-Maraver), Nonlinear Systems and Complexity, vol. 37, pp. 155–186. Switzerland: Springer Nature.
- 32. Deconinck B, McGill P, Segal BL. 2017 The stability spectrum for elliptic solutions to the sine-Gordon equation. *Phys. D* **360**, 17–35. (doi:10.1016/j.physd.2017.08.010)
- 33. Deconinck B, Segal BL. 2017 The stability spectrum for elliptic solutions to the focusing NLS equation. *Phys. D* **346**, 1–19. (doi:10.1016/j.physd.2017.01.004)
- 34. Deconinck B, Upsal J. 2020 The orbital stability of elliptic solutions of the focusing nonlinear Schrödinger equation. *SIAM J. Math. Anal.* **52**, 1–41. (doi:10.1137/19M1240757)
- 35. Upsal J, Deconinck B. 2020 Real Lax spectrum implies spectral stability. *Stud. Appl. Math.* **145**, 765–790. (doi:10.1111/sapm.12335)
- 36. Chen J, Pelinovsky DE. 2024 Rogue waves arising on the standing periodic waves in the Ablowitz–Ladik equation. *Stud. Appl. Math.* **152**, 147–173. (doi:10.1111/sapm.12634)
- 37. Chen J, Pelinovsky DE, Upsal J. 2021 Modulational instability of periodic standing waves in the derivative NLS equation. *J. Nonlin. Sci.* **31**, 58. (doi:10.1007/s00332-021-09713-5)
- 38. Chen J, Pelinovsky DE, White RE. 2020 Periodic standing waves in the focusing nonlinear Schrödinger equation: Rogue waves and modulation instability. *Phys. D* **405**, 132378. (doi:10.1016/j.physd.2020.132378)

- 39. Cui S, Pelinovsky DE. 2025 Stability of standing periodic waves in the massive Thirring model. *Stud. Appl. Math.* **154**, e12789. (doi:10.1111/sapm.12789)
- 40. Chen J, Pelinovsky DE. 2023 Periodic waves in the discrete mKdV equation: modulational instability and rogue waves. *Phys. D* **445**, 133652. (doi:10.1016/j.physd.2023.133652)
- 41. Pelinovsky DE. 2021 Instability of double-periodic solutions in the nonlinear Schrödinger equation. *Front Phys.* **9**, 599146. (doi:10.3389/fphy.2021.599146)
- 42. Ablowitz MJ, Kaup DJ, Newell AC, Segur H. 1974 The inverse scattering transform–Fourier analysis for nonlinear problems. *Stud. Appl. Math.* 53, 249–315. (doi:10.1002/sapm1974534249)
- 43. Kamchatnov AM. 1990 On improving the effectiveness of periodic solutions of the NLS and DNLS equations. *J Phys A: Math. Gen.* 23, 2945–2960. (doi:10.1088/0305-4470/23/13/031)
- 44. Kamchatnov AM. 1997 New approach to periodic solutions of integrable equations and nonlinear theory of modulational instability. *Phys. Rep.* **286**, 199–270. (doi:10.1016/S0370-1573(96)00049-X)
- 45. Kamchatnov AM, Spire A, Konotop VV. 2004 On dissipationless shock waves in a discrete nonlinear Schrödinger equation. *J. Phys. A: Math. Gen.* 37, 5547–5568. (doi:10.1088/0305-4470/37/21/004)
- 46. Kamchatnov AM, Kuo Y-H, Lin T-C, Horng T-L, Gou S-C, Clift R, El GA, Grimshaw RHJ. 2012 Undular bore theory for the Gardner equation. *Phys. Rev. E* **86**, 036605. (doi:10.1103/PhysRevE.86.036605)
- 47. Yang J. 2010 Nonlinear waves in integrable and non-integrable systems. Philadelphia, PA: SIMA.
- 48. Cui S, Pelinovsky DE. 2025 Instability bands for periodic travelling waves in the modified Korteweg–de Vries equation. Figshare. (doi:10.6084/m9.figshare.c.7947832)